https://doi.org/10.5194/egusphere-2025-2732
Preprint. Discussion started: 4 July 2025
© Author(s) 2025. CC BY 4.0 License.

China's Three Major Cereal Crops Exposure to Compound Drought and Extreme Rainfall Events

Hanming Cao[a] *, Qiren Yang[a]*, Wei Yang[a]*, Lin Zhao[a#]

[a] School of Resource and Environmental Sciences, Wuhan University, Wuhan 430079, China

Correspondence to: Lin Zhao (linzhao@whu.edu.cn)

Abstract

Under the backdrop of global climate change, the increasing intensity and frequency of anomaly climate events have led to a rise in compound extreme events. China's large population exacerbates the pressure of agricultural production, and compound drought and extreme rainfall events (CDER) can cause considerable damage to soil structure, thereby disrupting normal agricultural activities. Previous studies have revealed the impacts of the individual event, but the spatiotemporal characteristics of CDER and their effects on agricultural production remain obscure. This study focuses on compound disaster events in China's nine major agricultural regions, where drought and extreme rainfall events occur within 5 days. The results show that compound disasters are mainly concentrated in the northwest, southwest, and northern regions. The impact area of compound disasters is largest in summer, and the frequency and intensity of drought-rainfall events are higher than those of rainfall-drought events. Further analysis at the crop growth stage scale reveals the exposure of the three major cereal crops (rice, wheat, and maize) during their growth stage. The study reveals that maize generally has the highest and most variable disaster risk, rice has the lowest risk with minimal fluctuations, and wheat has moderate risk with large variations. The risk evolution in each agricultural region follows a universal pattern of "first rising and then declining", with the peak occurring around 2010. This study elucidates the spatiotemporal distribution patterns of this novel compound disaster and provides constructive insights for disaster prevention and mitigation through more refined risk assessments.

Keywords: *compound drought and extreme rainfall events; crop maturity exposure; nine major agricultural regions in China; spatiotemporal distribution characteristics*

*These authors contributed equally.
#Correspondence to: Lin Zhao (linzhao@whu.edu.cn)

https://doi.org/10.5194/egusphere-2025-2732
Preprint. Discussion started: 4 July 2025
© Author(s) 2025. CC BY 4.0 License.

1. Introduction

Climate change is one of the most serious threats to human society in the 21st century and may generate more extreme weather events and show an increasing trend at regional and global scales under anthropogenic climate change (AghaKouchak et al., 2014; Leonard et al., 2014; Zscheischler et al., 2020). With the intensification of global warming, the frequency, intensity, and compound effects of extreme rainfall and drought events have shown significant increases (Fang et al., 2025; Hao et al., 2018; Walz et al., 2021). The Sixth Assessment Report of the IPCC indicates that the frequency of compound drought and extreme rainfall events globally increased by 34% between 1980 and 2020 compared to pre-industrial levels (Anon, n.d.). Farmers are constantly dealing with and managing various agricultural risks that may have compound effects (Van Winsen et al., 2013; Wauters et al., 2014). Compound extreme events can exacerbate the damage caused by individual events and push global socio-economic systems to tipping points (Dickinson et al., 2016). This is because the combined stressors can overwhelm the capacity of exposed natural and human systems to cope with extreme conditions (Jayaraman et al., 2025; Ruess et al., 2025). The hazards of compound drought and extreme rainfall events (CDER) are not only reflected in the individual effects of drought or extreme rainfall but also in their combined effects. These events can cause significant damage to soil structure: extreme rainfall-induced soil erosion leads to an annual loss of 240 billion tons of topsoil globally (Borrelli et al., 2017), while anomaly drought can reduce soil organic matter content by 40-60%. Extreme rainfall events, characterized by high intensity and short duration, can induce severe soil erosion through processes such as splash erosion and overland flow (Quansah, 1981; Wang, et al., 2021). The resultant detachment and transport of soil particles not only degrade soil fertility but also contribute to sedimentation in water bodies, exacerbating water quality issues. This alarming rate of soil erosion underscores the vulnerability of agricultural lands and natural ecosystems to hydrological extremes. Conversely, prolonged drought conditions impose distinct yet equally detrimental impacts on soil structure (Vicente-Serrano et al., 2020). Droughts reduce soil moisture levels, which are critical for maintaining soil aggregate stability and porosity. The desiccation of soil organic matter (SOM) under drought stress leads to its accelerated decomposition, resulting in a significant reduction in SOM content—often by 40-60%

(Goebel et al., 2011; Yang and Liu, 2020). This decline in SOM not only diminishes soil fertility but also compromises the soil's ability to retain water and nutrients, further exacerbating its susceptibility to erosion during subsequent rainfall events. Additionally, drought-induced changes in soil structure can reduce hydraulic conductivity, impairing water infiltration and increasing runoff generation during rainfall events, and the water-replenishing effect of rainfall is further limited (Caplan et al., 2019).

The combined effect of these two factors can reduce soil productivity by up to 75% (Lal, 2015). Since the 1990s, the frequency of "drought-flood abrupt alternation" events in the South China and Southwest regions has significantly increased by over 40% (Hui et al., 2013; Shen, B.Z. et al., 2012; Wang, S. et al., 2009). These compound events pose a significant threat to China's agricultural production and ecological environment. Meanwhile, China, with only 7% of the world's arable land, must support 20% of the global population (Bongaarts, 2021). Moreover, the economic losses caused by these events are substantial and widespread. For example, in 2011, after experiencing continuous drought in winter, spring, and summer, the middle and lower reaches of the Yangtze River suffered from heavy rainfall, resulting in over 2 million hectares of affected cropland and direct economic losses of 29.36 billion yuan (Meteorological Publishing House, 2012). Against this backdrop, the urgency of enhancing agricultural climate resilience is highlighted.

Existing studies have focused on the phenomenon of drought and extreme rainfall alternation, but most compound event identification studies are limited to provincial scales rather than national scales (Barriopedro et al., 2011; Zhao et al., 2023). Some studies are motivated by the development of an integrated index to address the multidimensional nature of agricultural drought impacts, its spatial vulnerability perspective, and scale requirements (Murthy et al., 2015). Additionally, while some studies have quantified the risks of population and economic exposure to drought-flood abrupt alternation using shared socio-economic pathways (Meng, et al., 2024), the exposure risks of directly affected crops remain unclear. Most studies have used hydrological indices to characterize compound events, focusing on daily scales and using indices such as the standardized precipitation-evapotranspiration index. In contrast, this study uses soil moisture data to monitor compound events from an agricultural perspective rather than a hydrological one. Moreover, encountering compound events during critical crop phenological stages can amplify yield

https://doi.org/10.5194/egusphere-2025-2732
Preprint. Discussion started: 4 July 2025
© Author(s) 2025. CC BY 4.0 License.

losses by 3-5 times (Lesk et al., 2022). The impact of compound events on crops at different growth stages is significant, but current agricultural studies have focused more on the exposure analysis of individual extreme rainfall and drought events, with limited research on compound event exposure. From a developmental perspective, existing studies have identified and analyzed drought-flood abrupt alternation events in China from daily, monthly, and annual scales, forming four important research hotspots and frontiers: identification methods, causation analysis, evolution characteristics, and disaster damages (Shen et al., 2018; Yang and Liu, 2020). However, there is still a lack of comprehensive, national-scale analyses of secondary CDER in agricultural regions. The spatiotemporal distribution and evolution characteristics of drought-flood abrupt alternation events in China remain unclear, and research on crop exposure in the nine major grain-producing regions is still a blank space.

We define CDER as disaster events where drought and extreme rainfall occur within a 5-day interval. Specifically, these can be divided into compound extreme rainfall-drought events $CDER_{rd}$ (extreme rainfall followed by drought within 5 days) and compound drought-rainfall $CDER_{dr}$ (drought followed by extreme rainfall within 5 days). The research statistically analyzes the frequency, intensity, monthly changes, and annual changes of these two types of events to reveal their spatiotemporal distribution characteristics comprehensively. Additionally, this study innovatively calculates the exposure of China's three major agricultural products (maize, wheat, and rice) during their maturation periods. By focusing on the crop growth stage, the study refines exposure calculations and trend analyses will aid in better disaster prevention and mitigation efforts based on an understanding of these compound disasters.

2.Materials and Methods

2.1 Study Area

China's agricultural regions are vast and geographically diverse, encompassing nine major agricultural zones that include plains, mountains, basins, and plateaus. These regions are crucial for grain production and span from 3°51′N to 53°33′N and 73°33′E to 135°05′E. The climate types are complex and varied, including tropical monsoon, subtropical monsoon,

https://doi.org/10.5194/egusphere-2025-2732
Preprint. Discussion started: 4 July 2025
© Author(s) 2025. CC BY 4.0 License.

temperate monsoon, temperate continental, and alpine climates. Crop maturity systems range from one harvest per year to three harvests per year. The agricultural zoning data of China are derived from the China Agricultural Comprehensive Zoning Map released by the National Agricultural Commission (**Fig. 1**), where C1 represents the Northeast China Region; C2 represents the Inner Mongolia and Great Wall Contiguous Region; C3 represents the Gansu-Xinjiang Region; C4 represents the Huang-Huai-Hai Region; C5 represents the Loess Plateau Region; C6 represents the Qinghai-Tibet Region; C7 represents the Middle-Lower Yangtze River Region; C8 represents the Southwest China Region; and C9 represents the South China Region).

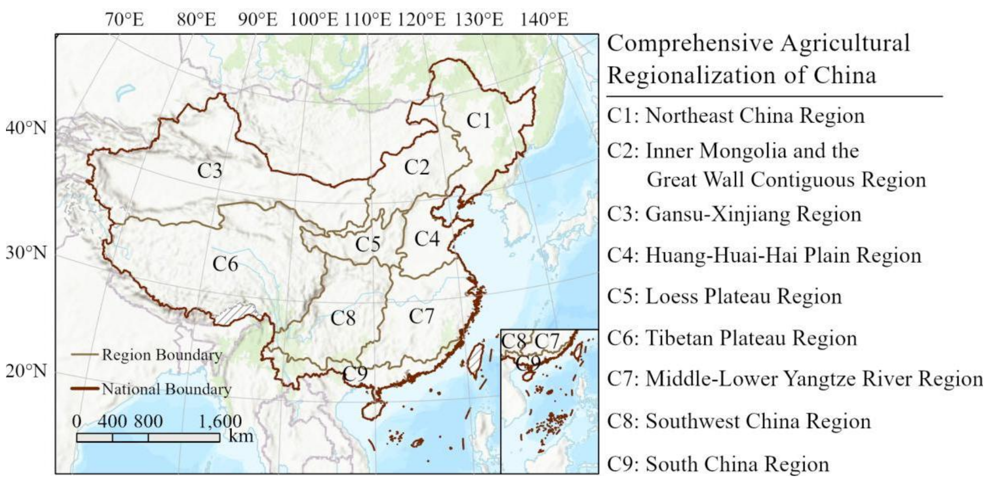

Fig.1 Agricultural Comprehensive Zoning(This map was created using Esri's ArcGIS® software. ArcGIS® and ArcMap™ are proprietary trademarks of Esri, used herein under license. © Esri. All rights reserved. For more information about Esri® software, please visit www.esri.com.)

2.2 Data

We utilized soil moisture data, precipitation data, and phenological data of the three major cereal crops. The soil moisture data were standardized to identify drought events; the 99th percentile of precipitation data for each grid cell with rainfall was set as the extreme rainfall threshold; and the phenological data of the crops were used to calculate the exposure during the maturity stage. The specific data details are as follows:

(1) China 1km Soil Moisture Daily Dataset (2000-2022) based on station observations.

https://doi.org/10.5194/egusphere-2025-2732
Preprint. Discussion started: 4 July 2025
© Author(s) 2025. CC BY 4.0 License.

National Tibetan Plateau Data Center. (https://cstr.cn/18406.11.Terre.tpdc.272415.)

(2) China Daily Precipitation Dataset (1961-2022): China Daily Precipitation Dataset (1961-2022, 0.1°/0.25°/0.5°): National Tibetan Plateau Data Center. (https://doi.org/10.11888/Atmos.tpdc.300523.https://cstr.cn/18406.11.Atmos.tpdc.300523.)

(3) National Three Major Grain Crops 1km Planting Distribution Dataset (2000-2019): Luo Yuchuan; Zhang Zhao. National Three Major Grain Crops 1km Planting Distribution Dataset [DS/OL]. National Ecological Science Data Center. (https://doi.org/10.12199/nesdc.ecodb.rs.2022.016.https://cstr.cn/15732.11.nesdc.ecodb.rs.2022.016.)

Table 1 Data Sources

Data Name	Time Span	Spatial resolution	Time resolution	Source
Soil Moisture	2000-2022	1km×1km	Daily	National Tibetan Plateau Data Center
Precipitation	1961-2022	9km×9km	Daily	National Tibetan Plateau Data Center
Crop Phenological Stages	2000-2019	1km×1km	Daily	National Ecological Science Data Center

2.3 Methodology

2.3.1 Identification of CDER

Compound events in this study are divided into two types: one is extreme rainfall followed by drought within 5 days ($CDER_{rd}$), and the other is drought followed by extreme rainfall within 5 days ($CDER_{dr}$) (Sun, et al., 2024). The intensity of compound drought and extreme rainfall events is composed of three parts: drought intensity, extreme rainfall intensity, and the interval time between the two events (**Eq. 1**). Extreme rainfall is defined as days with rainfall exceeding the 99th percentile threshold of the grid's rainfall days (Schillerberg and Tian, 2024). A drought event is defined as a day on which the standardized soil moisture index (SSMI) in the region falls below one negative standard deviation of the 21 years mean value of this index. All extreme rainfall events are standardized and shifted to

https://doi.org/10.5194/egusphere-2025-2732
Preprint. Discussion started: 4 July 2025
© Author(s) 2025. CC BY 4.0 License.

ensure values are greater than or equal to zero to obtain extreme rainfall intensity. Drought events are identified using the standardized soil moisture index, with the average value during the entire drought duration representing drought intensity.

$$C = \frac{P \times D}{\Delta t} \tag{1}$$

Here C represents the compound event intensity, P represents the extreme rainfall intensity, D represents the drought intensity, and Δt represents the interval time between extreme rainfall and drought events.

2.3.2 Mechanism of Soil Damage from CDER

Compound events involving drought and extreme rainfall exert synergistic negative impacts on soil health and agricultural productivity. Extreme rainfall events induce severe soil erosion, resulting in the loss of fine particles and essential nutrients. Simultaneously, prolonged drought conditions accelerate the decomposition and depletion of soil organic matter (SOM), further weakening soil structure. Together, these processes significantly increase soil erosion susceptibility. Drought-induced degradation of soil aggregate stability reduces porosity and water retention capacity. When followed by intense, short-duration rainfall, the already-compromised soil structure is further damaged by surface runoff and the destruction of soil pores, leading to a sharp decline in the infiltration rate. As a result, the limited water that is delivered during extreme rainfall events fails to effectively rehydrate the soil, compounding the water deficit stress experienced by crops and impairing agricultural resilience.

https://doi.org/10.5194/egusphere-2025-2732
Preprint. Discussion started: 4 July 2025
© Author(s) 2025. CC BY 4.0 License.

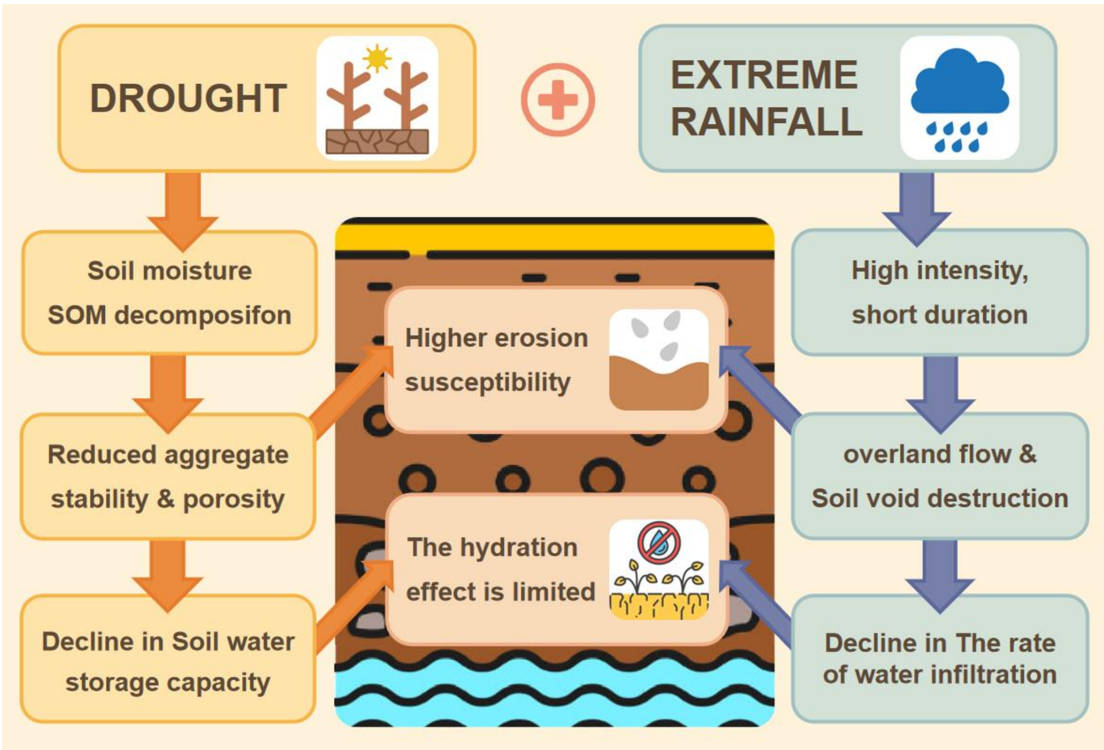

Fig.2 Schematic Diagram of Mechanism

2.3.3 Calculation of Crops Exposure to CDER

The exposure during the growth stage of each crop is calculated by multiplying the number of compound events occurring within the growth stage of each grid by the agricultural land area of that grid (**Eq. 2**). We use the crop maturity date in combination with the typical maturity period length of the three major crops to backtrack and determine the time window for the entire growing season, within which we count the occurrences of compound events to obtain *f*. Specifically, we select 130 days for maize, 100 days for rice, 300 days for winter wheat, and 100 days for spring wheat. In China, a large proportion of rice cultivation consists of double-cropping rice, which includes early rice and late rice. Due to its higher yield, better grain quality, greater economic value, and increased vulnerability to CDER, this study focuses exclusively on late rice.

$$Exp_{agr} = Agr \times f \tag{2}$$

© Author(s) 2025. CC BY 4.0 License.

Where f represents the frequency of compound events, Exp_{agr} represents the agricultural exposure, and Agr represents the agricultural land area.

2.3.4 Other Statistical Methods

This study employed several methods to analyze CDER. Soil moisture data are standardized to identify drought conditions by transforming them to a distribution with a mean of 0 and a standard deviation of 1. The Least Squares Method (LSM) is used to fit a linear trend and assess annual changes in the frequency of compound events. The K-Means clustering algorithm classifies event intensity into five levels based on data similarity. Loess regression is applied to model local trends in crop risk evolution, capturing non-linear patterns through weighted least squares within local neighborhoods. These approaches enabled a comprehensive analysis of extreme climate events in relation to crop phenology and soil moisture.

3.Result

3.1 Spatiotemporal Characteristics of CDER

The spatial distribution of the frequency and intensity of compound drought-rainfall and compound rainfall-drought events across China is shown in **Fig.3**. Overall, the frequency is higher in the northwest and southwest regions, particularly in the Hengduan Mountains and northern Xinjiang. The two types of compound disasters exhibit spatial heterogeneity. The high-intensity regions of compound drought-rainfall events are mainly concentrated in the northern areas, especially in parts of Northeast China and Inner Mongolia. In contrast, compound rainfall-drought events have high-intensity regions not only in the northeast but also in the south, particularly in South China and the Jianghuai region. Compared to CDER_{rd}, the frequency of CDER_{dr} is significantly higher.

https://doi.org/10.5194/egusphere-2025-2732
Preprint. Discussion started: 4 July 2025
© Author(s) 2025. CC BY 4.0 License.

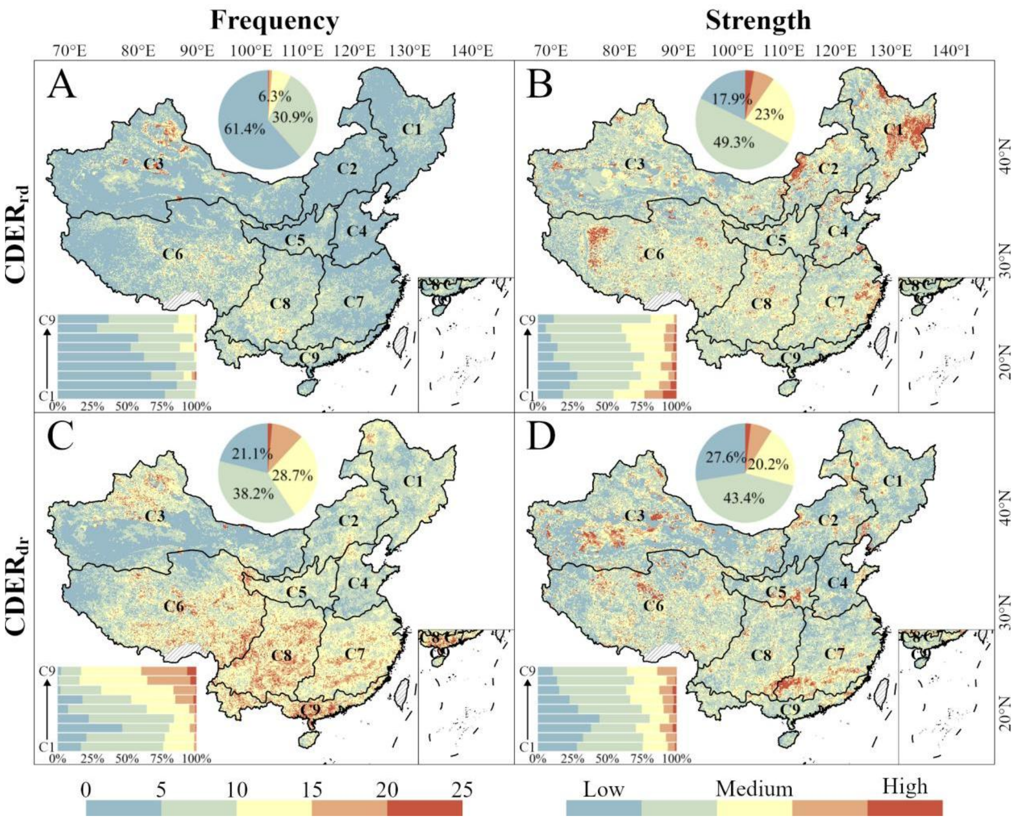

Fig.3 Spatial Distribution of Compound Drought and Extreme Rainfall Events(Figure A and B show the frequency and intensity of CDER$_{rd}$, respectively, while Figure C and D depict the frequency and intensity of CDER$_{dr}$. The bar charts represent the proportion of different color values within each region, while the pie charts show the proportion of each magnitude across the entire country.)

CDER$_{dr}$ and CDER$_{rd}$ exhibit distinct seasonal differences. The monthly average affected area of CDER$_{dr}$ and CDER$_{rd}$ in the nine agricultural regions is shown in **Fig. 4**. The temporal trends are similar across regions, with no significant inter-regional differences. Overall, CDER$_{dr}$ have the highest affected area during summer (June, July, and August), reaching over 20% of the total area. Each region's bar chart shows a unimodal distribution, with the northern regions (C1-C6) peaking in July and the southwest and south China regions (C7-C9) peaking in June. The affected area of CDER$_{dr}$ is almost zero from December to January, indicating that these events rarely occur in

https://doi.org/10.5194/egusphere-2025-2732
Preprint. Discussion started: 4 July 2025
© Author(s) 2025. CC BY 4.0 License.

winter and are mainly distributed in the middle and lower reaches of the Yangtze River, southwest, and south China regions.

Comparing the monthly changes in the affected areas of $\mathrm{CDER_{dr}}$ and $\mathrm{CDER_{rd}}$, both show consistent monthly trends, with the highest occurrence in summer, followed by spring and autumn, and almost no occurrence in winter. However, the affected area of $\mathrm{CDER_{dr}}$is significantly higher than that of $\mathrm{CDER_{rd}}$. The affected area of $\mathrm{CDER_{dr}}$ can reach up to 40%, while that of $\mathrm{CDER_{rd}}$ is around 20%. Overall, the affected area of $\mathrm{CDER_{dr}}$ is approximately twice that of $\mathrm{CDER_{rd}}$. Additionally, in C9, $\mathrm{CDER_{dr}}$ show a relatively high peak in July, while $\mathrm{CDER_{rd}}$ do not exhibit a significant peak.

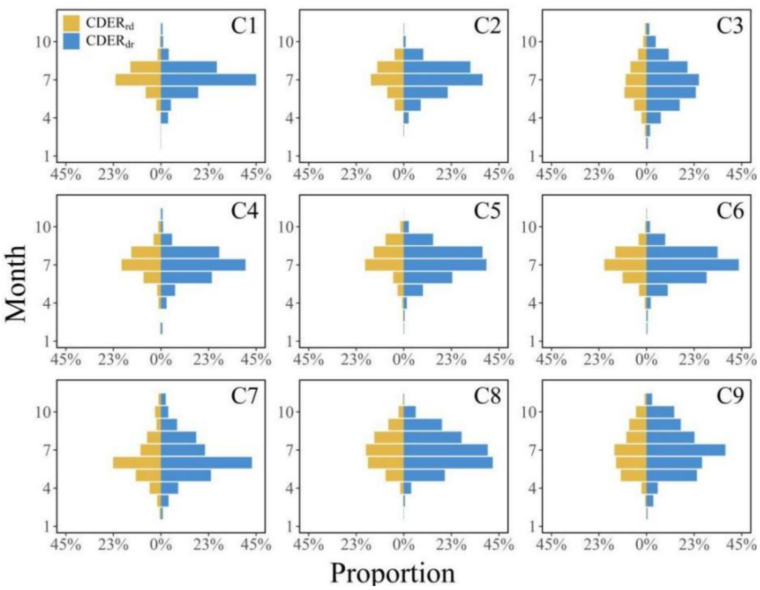

Fig.4 Monthly Average Affected Area of Compound Drought-Rainfall Events（C1 to C9 represent the nine major agricultural regions mentioned earlier, with yellow indicating $\mathrm{CDER_{rd}}$ and blue representing $\mathrm{CDER_{dr}}$）

The annual changes in the affected area of the two types of compound events show certain regional differences. This study further analyzes the annual trends in the affected area of the two types of events in the nine agricultural regions from 2000 to 2020 (**Fig. 5, Fig. 6**). The distribution patterns are similar across regions, with significant differences mainly in C1, C2, C3, C4 and C5. Both types of compound events show an increasing

https://doi.org/10.5194/egusphere-2025-2732
Preprint. Discussion started: 4 July 2025
© Author(s) 2025. CC BY 4.0 License.

trend in these regions, with compound rainfall-drought events increasing more significantly. However, in C3 and C4, a slight decreasing trend was observed from 2018 to 2020. $\mathrm{CDER_{dr}}$ only showed a significant increasing trend in C1, with no significant changes in other areas. In contrast, C7 and C9 showed a decreasing trend in both types of compound events, with $\mathrm{CDER_{rd}}$ decreasing more significantly. $\mathrm{CDER_{dr}}$ showed no significant trend in C7 amd C8, with a peak in 2014 and a slight rebound around 2019. C9 showed a fluctuating decreasing trend, with an upward trend after 2017. C6showed a unique pattern, with a decreasing trend in $\mathrm{CDER_{dr}}$ and an increasing trend in $\mathrm{CDER_{rd}}$.

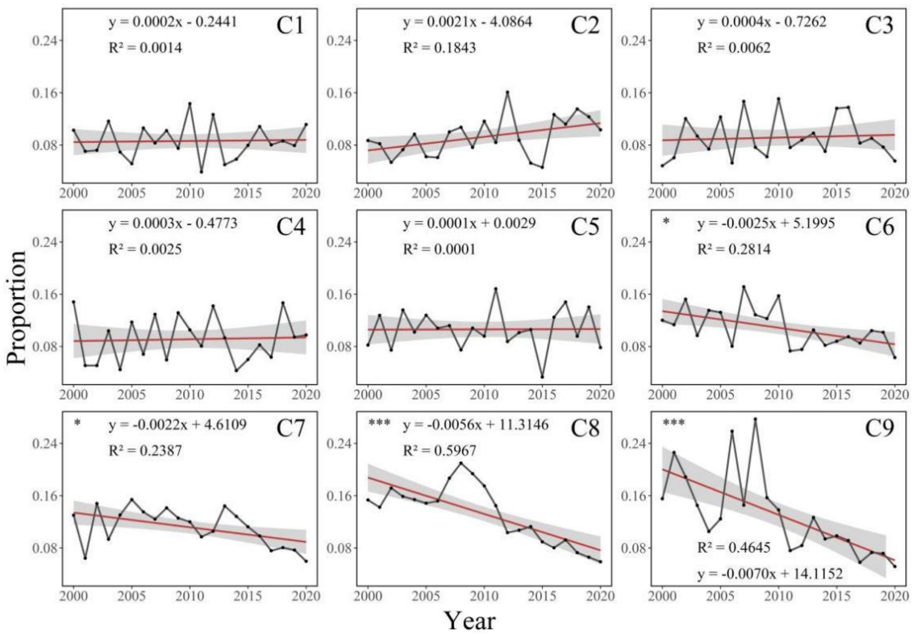

Fig. 5 Annual Frequency of Compound Drought-Rainfall Events (Red line represents the fitted trend line, and the shaded area represents the confidence interval. One star indicates $p < 0.05$, two stars indicate $p < 0.01$, and three stars indicate $p < 0.001$)

https://doi.org/10.5194/egusphere-2025-2732
Preprint. Discussion started: 4 July 2025
© Author(s) 2025. CC BY 4.0 License.

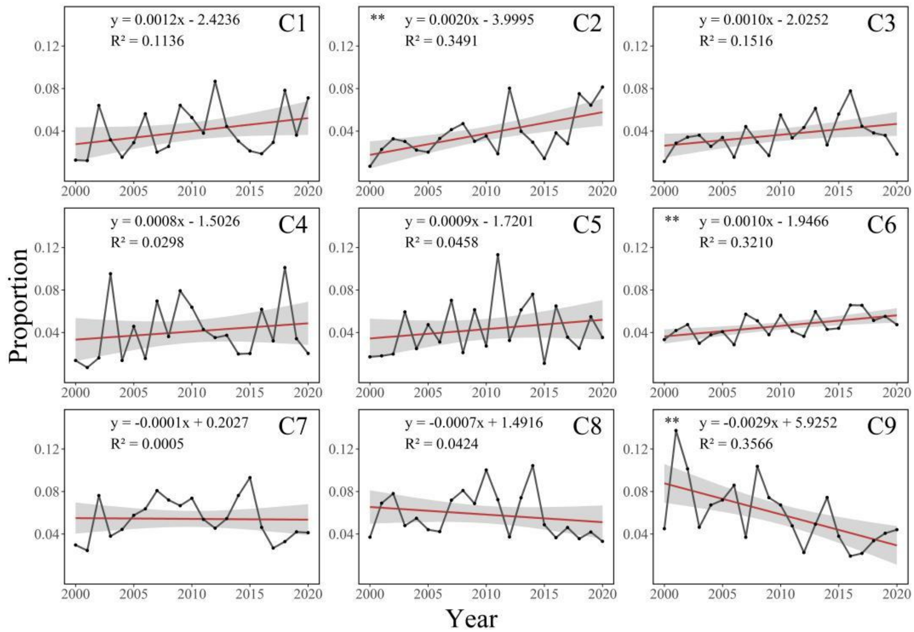

Fig. 6 Annual Frequency of Compound Rainfall-Drought Events (Red line represents the fitted trend line, and the shaded area represents the confidence interval. One star indicates $p < 0.05$, two stars indicate $p < 0.01$, and three stars indicate $p < 0.001$)

3.2 Agricultural Production Exposure Analysis

3.2.1 Spatial Distribution of Compound Event Risk in Nine Major Agricultural Regions

The boxplots of compound event risk for maize, rice, and wheat in the nine agricultural regions (**Fig. 7**) show significant differences in exposure across crops and regions, with noticeable fluctuations. Overall, C8 has the highest exposure for all crops, while regions with unique geographical environments, C1, C2, and C6, exhibit lower exposure. Among the three major crops, wheat has the highest average exposure, followed by maize, while rice has the lowest exposure due to its limited planting areas.

Specifically, maize has a high and highly variable disaster risk, particularly in C4 and C5. The high risk in these areas may be due to the large maize planting areas and frequent disaster occurrences, resulting in higher exposure. In contrast, rice has a lower exposure with minimal fluctuations, likely due to its growth adaptability and relatively

https://doi.org/10.5194/egusphere-2025-2732
Preprint. Discussion started: 4 July 2025
© Author(s) 2025. CC BY 4.0 License.

stable local climate conditions. Although C7, C8, and C9 have higher exposure, the fluctuations are small, indicating that the growth risks of rice in these regions are relatively manageable. Wheat has a moderate exposure with large variations, especially in C4 and C5. The exposure for wheat in these regions are more dispersed and show significant differences. Comparing the risks across regions, C1 and C6 have low disaster risks for all three crops, but the reasons are different. The Northeast has a suitable climate for crop growth and fewer disasters, while the Qinghai-Tibet Plateau has low crop planting areas. The C8 shows a moderate to high disaster risk, indicating that climate change and disaster occurrences in this region may have a certain impact on crop planting. Overall, crop disaster risks are closely related to regional climate characteristics. Maize faces higher disaster risks in regions with severe climate change, while rice is relatively stable, and wheat shows significant regional differences.

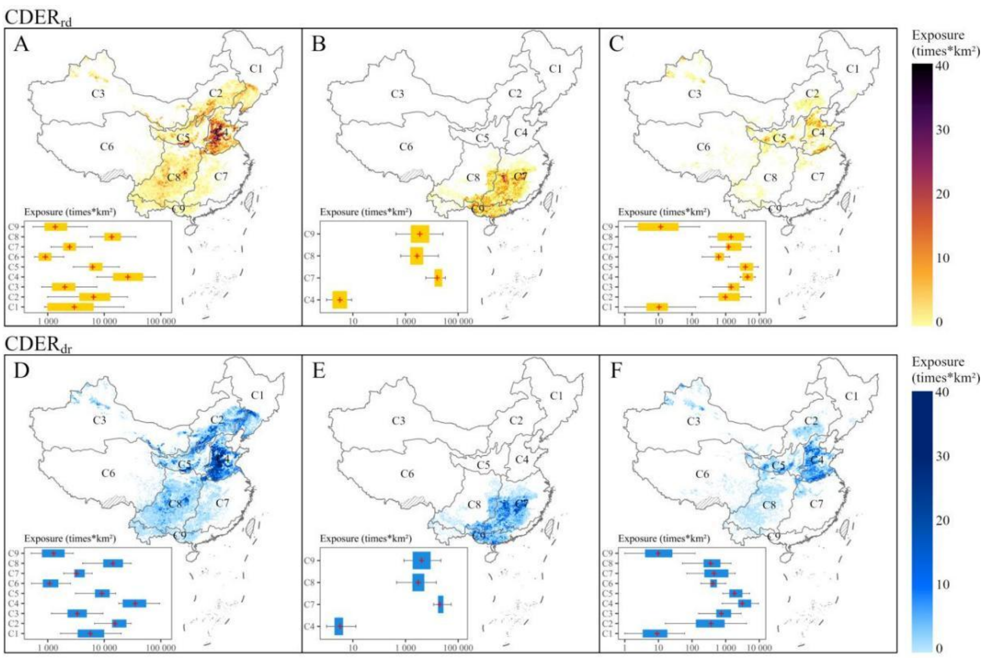

Fig. 7 Boxplots and Spatial Distribution Maps of Exposure Risk for the Three Major Crops in the Nine Agricultural Regions (A1, A2, A3 represent the exposure during CDER$_{rd}$ for maize, rice, and wheat, respectively; B1, B2, B3 represent the exposure during CDER$_{dr}$ for maize, rice, and wheat,The box plots display the distribution of exposure values across the different regions.)

https://doi.org/10.5194/egusphere-2025-2732
Preprint. Discussion started: 4 July 2025
© Author(s) 2025. CC BY 4.0 License.

3.2.2 Annual Changes in exposure of the Three Major Crops

Based on the exposure data of maize in the nine agricultural regions from 2000 to 2019, fitted curves were constructed (**Fig. 8**). Overall, the risk evolution in each agricultural region follows a universal pattern of "first rising and then declining," with the risk peak occurring around 2010. This is closely related to the high frequency and intensity of compound events in that year. Specifically, C1, C3, C5, and C7 show a three-stage characteristic of "rise-decline-rise." A significant trough was formed in 2013, followed by a risk rebound, especially in C5 and middle and lower reaches of C7. In contrast, C2, C4, C6, and C8 maintain a typical single-peak pattern, with no further breakthrough of the previous high point after 2010. Notably, C9 shows a unique trend of "first declining and then rising," which may be related to the expansion of maize planting areas in later years. In terms of regional risk levels, C4 has the highest risk value, followed by C2, C5, and C8, while C1, C3, C6, C7, and C9 have relatively lower risk values. Spatial heterogeneity analysis indicates that the differences in maize planting scales across agricultural regions are the key driving factors behind the formation of the risk distribution pattern.

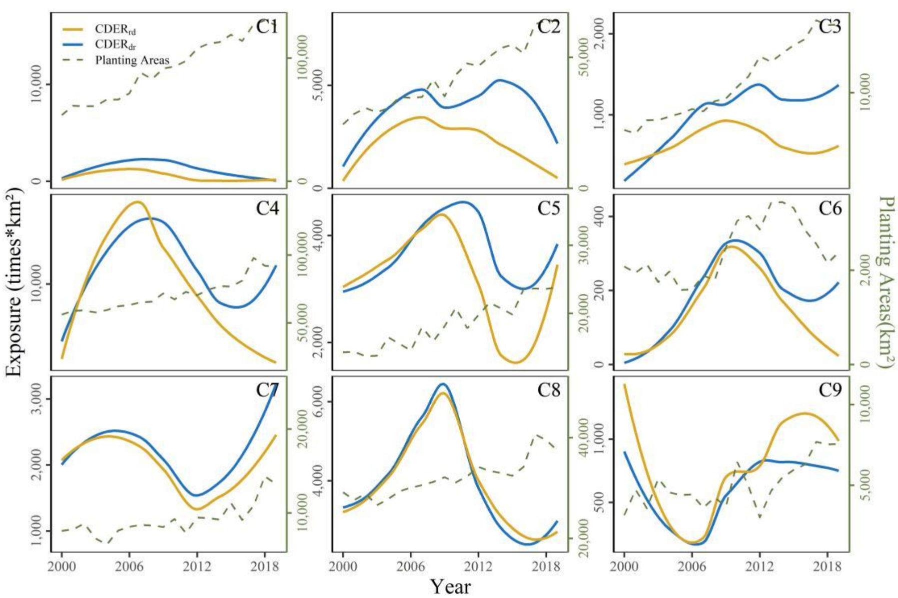

Fig. 8 Fitted Curve of Maize Exposure Risk During CDER$_{rd}$ in the Nine Agricultural

https://doi.org/10.5194/egusphere-2025-2732
Preprint. Discussion started: 4 July 2025
© Author(s) 2025. CC BY 4.0 License.

Regions (2000-2019) (The yellow curve represents the annual exposure trend for $CDER_{dr}$, the blue curve represents the annual exposure trend for $CDER_{rd}$, while the green line shows the annual variation in planting area.)

The fitted curves of rice exposure risk in the nine agricultural regions from 2000 to 2019 were plotted (**Fig. 9**). Overall, the disaster risk in most regions remained stable during this period, with no significant fluctuations or upward trends. Specifically, C1, C2, C3, C5, and C6 had no rice planting, and thus the exposure risk remained zero. C9 showed a unique change, with relatively uniform distribution of data points and a small variation in the fitted curve. Only in 2009 and 2014 were there noticeable exposure risks, and each time the risk value was relatively high. In contrast, C4 showed a trend of first rising, then falling, and rising again, with an overall upward trend in risk, indicating that this region faced higher disaster risks over the past 20 years. C7 showed a trend of first rising and then falling, while C8 showed certain fluctuations with both increases and decreases in risk, but the overall exposure risk tended to decline. In terms of regional risk levels, C7 had the highest risk value, while other agricultural regions had generally low exposure risks.

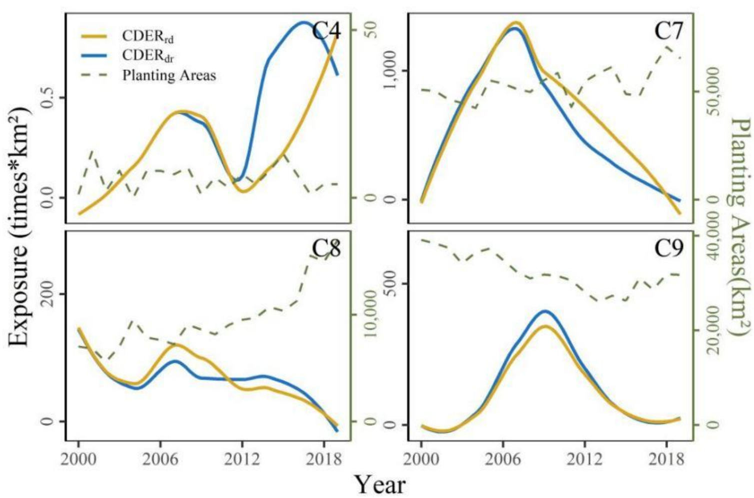

Fig. 9 Fitted Curve of Rice Exposure Risk During $CDER_{rd}$ in the Nine Agricultural Regions (2000-2019) (The yellow curve represents the annual exposure trend for $CDER_{dr}$, the blue curve represents the annual exposure trend for $CDER_{rd}$, while the green line shows the annual variation in planting area.)

https://doi.org/10.5194/egusphere-2025-2732
Preprint. Discussion started: 4 July 2025
© Author(s) 2025. CC BY 4.0 License.

The exposure risk of wheat in the nine agricultural regions from 2000 to 2019 was analyzed (**Fig. 10**). The results showed that the exposure risk of wheat remained stable in most agricultural regions. Specifically, C1, C2, C7, and C9 had almost zero exposure risk to compound events during the observation period. C1 had a slight risk value before 2010, which then completely declined to zero. C2, C7, C9 showed minor fluctuations but an overall decreasing trend in risk. Notably, C3 and C6 exhibited periodic fluctuations in exposure risk but remained at a basic risk threshold. C4 and C5 showed a significant "first rising and then declining" risk evolution pattern, with high risk indices. In terms of regional risk patterns, C4 had the highest risk index of 20,000, followed by C5 with 10,000, while other agricultural regions had risk values generally below 6,000. As the core wheat-producing regions in China, the high-risk characteristics of the Huang-Huai-Hai and the Loess Plateau regions are significantly correlated with regional agricultural planting scales. Similarly, the comparison of exposure risks between the two types of compound events revealed that the exposure risk caused by compound drought-rainfall events is almost twice that of compound rainfall-drought events.

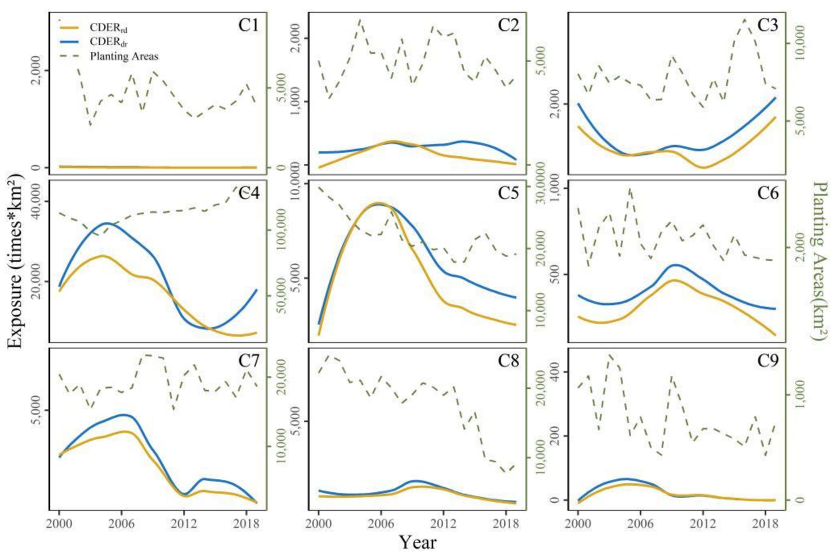

Fig. 10 Fitted Curve of Wheat Exposure Risk During CDER$_{rd}$ in the Nine Agricultural Regions (2000-2019) (The yellow curve represents the annual exposure trend for CDER$_{dr}$, the blue curve represents the annual exposure trend for CDER$_{rd}$, while the green line shows the annual variation in planting area.)

For all types of grain crops, the exposure risk caused by $CDER_{dr}$ is significantly higher than that caused by $CDER_{rd}$. However, this two-fold relationship is not always observed. The study found that in agricultural regions with larger crop planting areas, the ratio of exposure risk between the two types of compound events is closer to the two-fold relationship between the affected areas of drought-rainfall and rainfall-drought events. This phenomenon can be attributed to the geographical non-overlap between the occurrence of compound events and major crop planting areas. When the agricultural planting area expands, the spatial coupling degree between the compound event occurrence area and the crop planting area increases, leading to a gradual increase in exposure. Additionally, the blue lines reflecting the annual changes in crop planting areas in each agricultural region show two general scenarios when combined with the exposure risk calculation results: (1) Opposite trends, where an increase in planting area leads to a decrease in exposure risk or a decrease in planting area leads to an increase in exposure risk; (2) One remains stable while the other fluctuates, either with minimal changes in planting area but significant fluctuations in exposure or vice versa. Both scenarios suggest that the interannual changes in exposure risk are primarily the result of changes in compound drought and extreme rainfall events themselves.

4. Discussion

4.1 Consistency Analysis of the Spatiotemporal Characteristics of CDER

Numerous studies have focused on the distribution patterns and impacts of drought-flood abrupt alternation events. These events share similarities with the $CDER_{dr}$ studied here, but they are typically approached from a hydrological perspective using runoff data, whereas our study focuses on the agricultural system using soil moisture data. Moderate rainfall following drought generally has a positive impact on agricultural production and the ecological environment. However, if drought abruptly turns into flooding, it can exacerbate soil erosion and other disasters, causing more severe impacts on crops and worsening water quality (Bi, 2022; Huang et al., 2019; Shi et al., 2022). In the field of $CDER_{rd}$ and $CDER_{dr}$, previous studies have indicated that in the Yangtze River middle and lower reaches, the frequency of $CDER_{dr}$ is mainly concentrated in July and August each year, while the intensity

https://doi.org/10.5194/egusphere-2025-2732
Preprint. Discussion started: 4 July 2025
© Author(s) 2025. CC BY 4.0 License.

shows certain fluctuations. In the Jianghuai-Huai River Basin, the onset of the rainy season in drought-prone and semi-humid regions is delayed by 1–2 months compared to that in humid regions, making the semi-humid and humid areas high-incidence regions for drought-flood abrupt alternation events (Xue, et al., 2024). Additionally, studies in Fujian Province, China, have found that $CDER_{rd}$ occur more frequently in February, July, and August, while $CDER_{dr}$ have a higher occurrence rate from June to October (Zhang et al., 2018). These findings are highly consistent with our results, further validating the spatiotemporal distribution characteristics of compound events in these regions.

However, due to significant differences in the identification methods, definition criteria, and time scales used in different studies, some discrepancies inevitably exist in the results. The study shows that $CDER_{dr}$ have significantly higher frequency and intensity than $CDER_{rd}$, with values approximately twice as high. Some studies using surface runoff data or the standardized precipitation index as indicators of compound events have found that the frequency and intensity of drought-flood and flood-drought events are comparable. Moreover, several scholars have explored the correlation between drought-flood abrupt alternation events and complex climate factors (Bian, 2023; Wang, et al., 2024), but the specific physical mechanisms behind these events are still under investigation, with no unified conclusions yet formed.

4.2 Uncertainty in the Impact of CDER on Crop Growth Stages

This study focuses on the maturity months of the three major grain crops and uses the monthly frequency of $CDER_{rd}$ and $CDER_{dr}$, along with 1km spatial resolution crop planting data, to characterize the exposure scenarios of the three major grain crops during their maturation periods in China's nine agricultural regions. Previous studies on crop exposure have mostly used annual time scales, such as those calculating exposure of population and farmland on a global scale for historical and future periods (2005 and 2085) (Tabari and Willems, 2023). However, disaster occurrences throughout the year do not always coincide with agricultural activities, leading to overestimation of crop exposure. Our study, which refines the exposure assessment to the crop maturity period, overcomes this limitation and provides a more accurate exposure profile.

Studies have shown that drought stress significantly affects crop yield, with varying impacts on different growth stages and species. For rice, drought during the reproductive stage causes a greater yield reduction compared to the early stages(Boonjung and Fukai et al., 1996). Similarly, wheat shows continuous yield reductions throughout its growth cycle. Maize is also more severely affected during the reproductive stage, with early-stage stress causing lasting damage to photosynthetic capacity(Daryanto et al., 2016; Ma et al., 2017). Overall, maize appears to be more sensitive to drought than wheat, with yield reductions of 39.3% and 20.6%, respectively, under 40% water reduction(Daryanto et al., 2016). Therefore, failing to consider the sensitivity of different growth stages of crops to compound drought and extreme rainfall events can lead to overestimation or underestimation of risks. We suggest that future research should focus on designing experiments or other forms of investigation to explore the sensitivity of different growth stages of the three major grain crops to compound disasters. Based on this, key growth stages should be identified to incorporate the vulnerability of the affected bodies into more refined exposure risk studies.

5. Conclusions

This study defines compound drought and extreme rainfall events, including $CDER_{dr}$ and $CDER_{rd}$, and analyzes their spatiotemporal distribution in China's nine major agricultural regions. High-intensity $CDER_{dr}$ are concentrated in the north, especially Northeast China and Inner Mongolia, while $CDER_{rd}$ are widespread in the northeast and south, particularly South China and the Jianghuai region. $CDER_{dr}$ occur with higher frequency and intensity, affecting up to 40% of the area, compared to 20% for $CDER_{rd}$. Both event types are most prevalent in summer, with regional differences observed in annual affected area changes, especially in the Northeast, Inner Mongolia, Great Wall, Gansu-Xinjiang, Huang-Huai-Hai, and Loess Plateau regions.

The study further refines the calculation of exposure to compound events for maize, rice, and wheat during their crop maturity periods. Results show significant regional differences in disaster risk, with C8 facing the highest risk for all crops, while regions like C1, C2, and C6 experience lower risks. Among the crops, wheat faces the highest risk, followed by maize, while rice has the lowest exposure due to limited planting areas. The risk evolution across regions follows a common pattern of rising and then declining, with a peak around 2010,

https://doi.org/10.5194/egusphere-2025-2732
Preprint. Discussion started: 4 July 2025
© Author(s) 2025. CC BY 4.0 License.

coinciding with higher frequencies and intensities of compound events.

Data availability

(1) China 1km Soil Moisture Daily Dataset (2000-2022) based on station observations. National Tibetan Plateau Data Center. (https://cstr.cn/18406.11.Terre.tpdc.272415.)

(2) China Daily Precipitation Dataset (1961-2022): China Daily Precipitation Dataset (1961-2022, 0.1°/0.25°/0.5°): National Tibetan Plateau Data Center. (https://doi.org/10.11888/Atmos.tpdc.300523.https://cstr.cn/18406.11.Atmos.tpdc.300523.)

(3) National Three Major Grain Crops 1km Planting Distribution Dataset (2000-2019): Luo Yuchuan; Zhang Zhao. National Three Major Grain Crops 1km Planting Distribution Dataset [DS/OL]. National Ecological Science Data Center. (https://doi.org/10.12199/nesdc.ecodb.rs.2022.016.https://cstr.cn/15732.11.nesdc.ecodb.rs.2022.016.)

Author contribution

Hanming Cao: Writing-original draft, Writing-review & editing, Conceptualization, Data curation, Investigation, Methodology, Validation. **Qiren Yang:** Writing-review & editing, Conceptualization, Visualization. **Wei Yang:** original draft & editing, Data curation, Methodology. **Lin Zhao:** Writing–review & editing, Funding acquisition, Project administration, Resources.

Competing interests

The contact author has declared that none of the authors has any competing interests.

Acknowledgments

This research was funded by Third Xinjiang Scientific Expedition Program (2022xjkk0601), National Natural Science Foundation of China (42471085 and U22B2011),

https://doi.org/10.5194/egusphere-2025-2732
Preprint. Discussion started: 4 July 2025
© Author(s) 2025. CC BY 4.0 License.

Natural Science Foundation of Hubei Province (2023AFB823).

References

AghaKouchak, A., Cheng, L., Mazdiyasni, O., and Farahmand, A.: Global warming and changes in risk of concurrent climate extremes: Insights from the 2014 California drought, Geophysical Research Letters, 41, 8847–8852, https://doi.org/10.1002/2014GL062308, 2014.

Anon: Sixth Assessment Report — IPCC, n.d.

Barriopedro, D., Fischer, E. M., Luterbacher, J., Trigo, R. M., and García-Herrera, R.: The Hot Summer of 2010: Redrawing the Temperature Record Map of Europe, Science, 332, 220–224, https://doi.org/10.1126/science.1201224, 2011.

Bi, W. X.: Soil phosphorus loss increases under drought-flood abrupt alternation in summer maize planting area, Agricultural Water Management, 2022.

Bian, Q.: Study on the sharp turn of drought and flood in summer and atmospheric circulation characteristics in typical years in Liangshan Prefectur, Journal of Mountain Meteorology, 47, 31-37 (in Chinese), 2023.

Bongaarts, J.: FAO, IFAD, UNICEF, WFP and WHOThe State of Food Security and Nutrition in the World 2020. Transforming food systems for affordable healthy dietsFAO, 2020, 320 p., Population & Development Rev, 47, 558–558, https://doi.org/10.1111/padr.12418, 2021.

Borrelli, P., Robinson, D. A., Fleischer, L. R., Lugato, E., Ballabio, C., Alewell, C., Meusburger, K., Modugno, S., Schütt, B., Ferro, V., Bagarello, V., Oost, K. V., Montanarella, L., and Panagos, P.: An assessment of the global impact of 21st century land use change on soil erosion, Nat Commun, 8, 2013, https://doi.org/10.1038/s41467-017-02142-7, 2017.

Caplan, J. S., Giménez, D., Hirmas, D. R., Brunsell, N. A., Blair, J. M., and Knapp, A. K.: Decadal-scale shifts in soil hydraulic properties as induced by altered precipitation, Sci. Adv., 5, eaau6635, https://doi.org/10.1126/sciadv.aau6635, 2019.

Daryanto, S., Wang, L., and Jacinthe, P.-A.: Global Synthesis of Drought Effects on Maize and Wheat Production, PLoS ONE, 11, e0156362, https://doi.org/10.1371/journal.pone.0156362, 2016.

Dickinson, C., Aitsi-Selmi, A., Basabe, P., Wannous, C., and Murray, V.: Global Community of Disaster Risk Reduction Scientists and Decision Makers Endorse a Science and Technology Partnership to Support the Implementation of the Sendai Framework for Disaster Risk Reduction 2015–2030, Int J Disaster Risk Sci, 7, 108–109, https://doi.org/10.1007/s13753-016-0080-y, 2016.

Fang, Z., Morales, A. B., Wang, Y., and Lombardo, L.: Climate change has increased rainfall-induced landslide damages in central China, International Journal of Disaster Risk Reduction, 119, 105320, https://doi.org/10.1016/j.ijdrr.2025.105320, 2025.

Goebel, M.-O., Bachmann, J., Reichstein, M., Janssens, I. A., and Guggenberger, G.: Soil water repellency and its implications for organic matter decomposition – is there a link to extreme climatic events?, Global Change Biology, 17, 2640–2656, https://doi.org/10.1111/j.1365-2486.2011.02414.x, 2011.

https://doi.org/10.5194/egusphere-2025-2732
Preprint. Discussion started: 4 July 2025
© Author(s) 2025. CC BY 4.0 License.

Hao, Z., Hao, F., Singh, V. P., and Zhang, X.: Changes in the severity of compound drought and hot extremes over global land areas, Environ. Res. Lett., 13, 124022, https://doi.org/10.1088/1748-9326/aaee96, 2018.

Huang, J., Hu, T., Yasir, M., Gao, Y., Chen, C., Zhu, R., Wang, X., Yuan, H., and Yang, J.: Root growth dynamics and yield responses of rice (Oryza sativa L.) under drought—Flood abrupt alternating conditions, Environmental and Experimental Botany, 157, 11–25, https://doi.org/10.1016/j.envexpbot.2018.09.018, 2019.

Hui, H., Peslier, A. H., Zhang, Y., and Neal, C. R.: Water in lunar anorthosites and evidence for a wet early Moon, Nature Geosci, 6, 177–180, https://doi.org/10.1038/ngeo1735, 2013.

Jayaraman, P., Jones, E. C., Stewart, H. L., and McCurdy, S.: The relationship of prior flood experience to posttraumatic stress and depression in minority communities after Hurricane Harvey, International Journal of Disaster Risk Reduction, 117, 105178, https://doi.org/10.1016/j.ijdrr.2025.105178, 2025.

Lal, R.: Restoring Soil Quality to Mitigate Soil Degradation, Sustainability, 7, 5875–5895, https://doi.org/10.3390/su7055875, 2015.

Leonard, M., Westra, S., Phatak, A., Lambert, M., Van Den Hurk, B., McInnes, K., Risbey, J., Schuster, S., Jakob, D., and Stafford-Smith, M.: A compound event framework for understanding extreme impacts, WIREs Climate Change, 5, 113–128, https://doi.org/10.1002/wcc.252, 2014.

Lesk, C., Anderson, W., Rigden, A., Coast, O., Jägermeyr, J., McDermid, S., Davis, K. F., and Konar, M.: Compound heat and moisture extreme impacts on global crop yields under climate change, Nat Rev Earth Environ, 3, 872–889, https://doi.org/10.1038/s43017-022-00368-8, 2022.

Ma, J., Li, R., Wang, H., Li, D., Wang, X., Zhang, Y., Zhen, W., Duan, H., Yan, G., and Li, Y.: Transcriptomics Analyses Reveal Wheat Responses to Drought Stress during Reproductive Stages under Field Conditions, Front. Plant Sci., 8, 592, https://doi.org/10.3389/fpls.2017.00592, 2017.

Meng, C. Q., Dong, Z. J., Wang, Y. K., Zhang, Y. Q., and Zhong, D. Y.: Evolution characteristics of drought-flood abrupt alternation events in Yangtze River basin and its socio-economic exposure, Journal of Hydroelectric Engineering, 43, 34–49, https://doi.org/10.11660/slfdxb.20240404 (in Chinese), 2024.

Meteorological Publishing House: China Meterological Administration. Yearbook of Meteorological Disasters in China, 2012.

Murthy, C. S., Laxman, B., and Sesha Sai, M. V. R.: Geospatial analysis of agricultural drought vulnerability using a composite index based on exposure, sensitivity and adaptive capacity, International Journal of Disaster Risk Reduction, 12, 163–171, https://doi.org/10.1016/j.ijdrr.2015.01.004, 2015.

Quansah, C.: THE EFFECT OF SOIL TYPE, SLOPE, RAIN INTENSITY AND THEIR INTERACTIONS ON SPLASH DETACHMENT AND TRANSPORT, Journal of Soil Science, 32, 215–224, https://doi.org/10.1111/j.1365-2389.1981.tb01701.x, 1981.

Ruess, P. J., Khalid, Z., Ferreira, C. M., and Kinter, J. L.: Social and environmental justice implications of flood-related road closures in Virginia, International Journal of Disaster Risk Reduction, 117, 105123, https://doi.org/10.1016/j.ijdrr.2024.105123, 2025.

Schillerberg, T. A. and Tian, D.: Global Assessment of Compound Climate Extremes and Exposures of

https://doi.org/10.5194/egusphere-2025-2732
Preprint. Discussion started: 4 July 2025
© Author(s) 2025. CC BY 4.0 License.

Population, Agriculture, and Forest Lands Under Two Climate Scenarios, Earth's Future, 12, e2024EF004845, https://doi.org/10.1029/2024EF004845, 2024.

Shen, B.Z., Zhang, S.X., Yang, H.W., Wang, K., and Feng, G.L.: Analysis of characteristics of a sharp turn from drought to flood in the middle and lower reaches of the Yangtze River in spring and summer in 2011, Acta Phys. Sin., 61, 109202–109202, https://doi.org/10.7498/aps.61.109202 (in Chinese), 2012.

Shen, S., Cheng, C., Yang, J., and Yang, S.: Visualized analysis of developing trends and hot topics in natural disaster research, PLoS ONE, 13, e0191250, https://doi.org/10.1371/journal.pone.0191250, 2018.

Shi, W., Huang, S., Zhang, K., Liu, B., Liu, D., Huang, Q., Fang, W., Han, Z., and Chao, L.: Quantifying the superimposed effects of drought-flood abrupt alternation stress on vegetation dynamics of the Wei River Basin in China, Journal of Hydrology, 612, 128105, https://doi.org/10.1016/j.jhydrol.2022.128105, 2022.

Sun, J. H., Su, B., Wang D. F., Huang J. L., Wang, B. W., Dai, R., and Jiang, T.: Temporospatial characteristics of drought-flood abrupt alteration events in China, Water Resources and Hydropower Engineering, 55, 13–23, https://doi.org/10.13928/j.cnki.wrahe.2024.08.002, 2024.

Tabari, H. and Willems, P.: Global risk assessment of compound hot-dry events in the context of future climate change and socioeconomic factors, npj Clim Atmos Sci, 6, 74, https://doi.org/10.1038/s41612-023-00401-7, 2023.

Van Winsen, F., De Mey, Y., Lauwers, L., Van Passel, S., Vancauteren, M., and Wauters, E.: Cognitive mapping: A method to elucidate and present farmers' risk perception, Agricultural Systems, 122, 42–52, https://doi.org/10.1016/j.agsy.2013.08.003, 2013.

Vicente-Serrano, S. M., Quiring, S. M., Peña-Gallardo, M., Yuan, S., and Domínguez-Castro, F.: A review of environmental droughts: Increased risk under global warming?, Earth-Science Reviews, 201, 102953, https://doi.org/10.1016/j.earscirev.2019.102953, 2020.

Walz, Y., Janzen, S., Narvaez, L., Ortiz-Vargas, A., Woelki, J., Doswald, N., and Sebesvari, Z.: Disaster-related losses of ecosystems and their services. Why and how do losses matter for disaster risk reduction?, International Journal of Disaster Risk Reduction, 63, 102425, https://doi.org/10.1016/j.ijdrr.2021.102425, 2021.

Wang, S., Tian, H., Ding, X. J., Xie, W. S., and Tao, Y.: Climate Characteristics of Precipitation and Phenomenon of Drought-flood Abrupt Alternation during Main Flood Season in Huaihe River Basin, Chinese Journal of Agrometeorology, 30, 31 (in Chinese), 2009.

Wang, X. J., Hua, X. Y., and Tian, F. C.: Study on the Spatiotemporal Variation Characteristics and Driving Forces of Drought–Flood Abrupt Alternation in Hainan Island from 1951 to 2020, qhyhjyj, 30, 1–14, https://doi.org/10.3878/j.issn.1006-9585.2024.23115 (in Chinese), 2024.

Wang, X. W., Li, L., Ding, Y. B., Xu, J. T., Wang, Y. F., Zhu, Y., Wang, X. Y., and Cai, H. J.: Adaptation of winter wheat varieties and irrigation patterns under future climate change conditions in Northern China, Agricultural Water Management, 243, 106409, https://doi.org/10.1016/j.agwat.2020.106409, 2021.

Wauters, E., Van Winsen, F., De Mey, Y., and Lauwers, L.: Risk perception, attitudes towards risk and risk management: evidence and implications, Agric. Econ. - Czech, 60, 389–405,

https://doi.org/10.5194/egusphere-2025-2732
Preprint. Discussion started: 4 July 2025
© Author(s) 2025. CC BY 4.0 License.

https://doi.org/10.17221/176/2013-AGRICECON, 2014.

Xue, L. Q., Zhang, Y. H., and Liu, Y. H.: Comparative study on change characteristics of drought-flood abrupt alternation in arid and humid zones, Water Resources Protection, 40, 1-8. (in Chinese), 2024.

Yang, T. H. and Liu, W. C.: A General Overview of the Risk-Reduction Strategies for Floods and Droughts, Sustainability, 12, 2687, https://doi.org/10.3390/su12072687, 2020.

Zhang, J., Zhang, S., Cheng, M., Jiang, H., Zhang, X., Peng, C., Lu, X., Zhang, M., and Jin, J.: Effect of Drought on Agronomic Traits of Rice and Wheat: A Meta-Analysis, IJERPH, 15, 839, https://doi.org/10.3390/ijerph15050839, 2018.

Zhao, Y., He, F., He, G. H., and Li, H. R.: Ten insights and reflections on the planning and construction of the national water network, China Water Resources, 23, 37–48, 2023.

Zscheischler, J., Martius, O., Westra, S., Bevacqua, E., Raymond, C., Horton, R. M., Van Den Hurk, B., AghaKouchak, A., Jézéquel, A., Mahecha, M. D., Maraun, D., Ramos, A. M., Ridder, N. N., Thiery, W., and Vignotto, E.: A typology of compound weather and climate events, Nat Rev Earth Environ, 1, 333–347, https://doi.org/10.1038/s43017-020-0060-z, 2020.